Finite Element Analysis of Broken Bars Fault in Induction Motor

A. Zorig and H. Radjeai

Department of Electrical Engineering, Setif University, Email: zorig_assam@yahoo.fr

Abstract—the paper presents the application of a finite element method for predicting the performance of induction motor having broken rotor bars. The detailed insight in magnetic field distribution of a squirrel cage induction motor forms the basis for further evaluation of its operational behavior. Increasing anomaly in magnetic field distribution due to the increasing number of broken rotor bars results in a degradation of steady-state and dynamic performance of induction motor and can be determined with computer simulation eliminating expensive and time consuming laboratory tests. Correct evaluation of faulty motor performance is very significant part of condition monitoring and diagnostic procedure in modern supervision systems of electrical drives.

Keywords– Induction Motor, Finite Element Method, Diagnostics.

I. INTRODUCTION

Fault diagnosis methods are widely utilized for maintenance and protection of induction motors. The principle of any reliable fault recognition technique is steady-state analysis of electrical, magnetic and mechanical behavior of the machine under fault conditions; modeling is the first step for studying this phenomenon. Generally, there are three major methods for fault analysis in induction motors. These are the magnetic equivalent circuit (MEC), winding function (WF) and finite element (FE) methods. In the MEC method, the equivalent magnetic circuit for each part of the motor is represented and these circuits are then connected to each others taking into account the direction of the magnetic flux.

It is noted that the complexity of precise mathematical models for induction motors is always the most difficult problem in the fault diagnosis. Simple models such as the MEC or d-q-o are unable to take into account the real fault cases [1]. The WF is a powerful technique that uses electrical circuits coupled to magnetic circuits and linking the relationship between the loop fluxes, stator winding currents, rotor bars current and voltages of the motor [2]. However, it is not possible to estimate the core losses of induction motor using this technique under faulty conditions. The FE method enables one to calculate the magnetic field distribution within the motor using its exact geometry and magnetic characteristics. Knowing the magnetic field distribution, other quantities of the motor such as induced voltage waveform, air gap magnetic flux density and different inductances can be obtained [3].
The finite element method has been used to analyze and diagnose a faulty induction motor [4]. Meanwhile, in this method, FEM is only used for inductance computations and the remaining calculations and analysis are carried out in a state-space environment.

Using FEM analysis the changes in electric, magnetic and mechanic behaviour of the machine due to any fault can be easily observed without the need of opening the machine, or experimenting in laboratories. The main idea is to understand the electric, magnetic and mechanical behaviour of the machine in its healthy state and under fault conditions,[5].

II. FEM MODEL OF THE INDUCTION MACHINE

In recent years the Finite Element Method (FEM) become widely used in the design and analysis of electric machines and of her electromagnetic devices. So far a lot of program packages for computation of magnetic field, especially for two dimensional (2D) analyses have been developed. This method it is based on Maxwell's equations for magnetic and electric field [6]:

$$\nabla \times \vec{H} = \vec{J} \text{ And } \nabla \times \vec{E} \quad -\frac{d\vec{B}}{dt} \qquad (1)$$

Where $\vec{H}$ is the magnetic field strength [A/m], $\vec{E}$ is the electric field strength [V/m], $\vec{J}$ is the electric current density [A/m], $\vec{B}$ is the magnetic flux density [T]. Moreover the electric and magnetic field quantities are related with the material properties expressed by the following relations.

$$\vec{J} = \sigma \vec{E} \text{ and } \vec{B} = \mu \vec{H}$$

Where σ the electrical conductivity [S/m], μ is the magnetic permeability [H/m].

Based on these equations FEM based programs compute the magnetic field distribution of any electrical machine. In the case of the 2D analysis the computations are performed for a transversal plane to the axes of the machine. Well-developed fault detection of any electrical machine requires a well-grounded theoretical basis. The use of simulation tools helps the researchers to emphasis the effects caused by faults in an electrical machine and to develop efficient fault detection methods. Using FEM analysis the changes in electric, magnetic and mechanic behavior of the machine due to any fault can be easily observed without the need of destroying a machine, or experimenting in laboratories machines with different fault types. The main idea was to understand the electric, magnetic and mechanical behavior of the machine in the healthy state and under fault condition.

To perform the FEM analysis of the induction machine Flux2D Simulation Software was used. This program is one of the best electromagnetic field simulation software worldwide used by hundreds of engineers and designers to design and analyze electromagnetic devices.

To build any simulation model in Flux2D, only a few steps have to be done. In the first step the geometrical model has to be created, on which the boundary conditions will be set up. Next the circuit model has to be created. The program automatically generates the mesh and start to solve the problem in concordance with the solver's parameters, which can be set up by the user. The field quantities can be visualized on the surface or a specified internal cross section of the component.

The squirrel-cage induction machine in study was of 7.5 kW rated power.

After the above-mentioned steps in creating the model, the automatic generated finite element mesh had to be corrected manually near the air-gap, where the magnetic flux has the highest gradient, in order to get the most accurate results in the area. A part of the corrected mesh is given in Fig. 1**.**

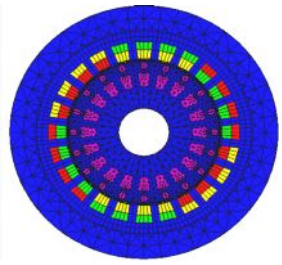

Fig.1. the solution meshes of the 2D FEM model of the induction machine.

Following a Circuit model has to be created, which permits to connect the coils to the source in order to properly simulate the voltage and current present at its terminals. In this way is possible to connect the coils to each other and to any other external circuit containing resistors, capacitors, inductors different types of current and voltage sources.

The circuit components presented in Fig.2 are as follows:

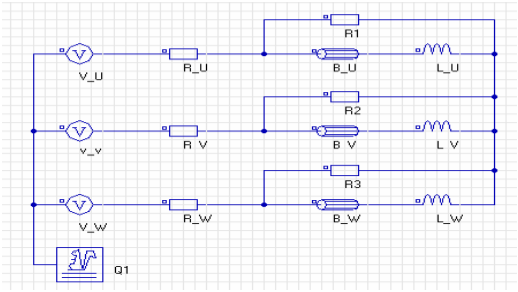

Fig.2. Circuit model of the squirrel cage induction

The circuit components "outside" the motor, for the applications with an imposed voltage source, Fig.2, are:

- Three voltage sources, V_U, V_V, V_W characterized by: RMS value U_{1n} = 380 V, frequency f_{1n} = 50 Hz.
- Three resistors, *R_U, R_V, R_W of 0.9 Ω* to model the voltage drop inside the power source network in the no-load motor start-up simulation and motor transient after the application of rated load. For the other magneto-dynamic and transient applications, these resistors have a very small resistance, 10^{-6} Ω.
- B_U, B_V, B_W represent the coils of the three-phase winding of the machine;
- L_U, L_V and L_W symbolize the stator end winding inductance per phase.
- a resistance of high value R1 = R2 = R3=10^6 , modeling the voltmeters that measure the phase to null voltage at the stator winding terminals;
- Q1 is a macro-circuit (a feature of Flux software package) used to model the squirrel cage of the machine [7].

III. SIMULATION RESULTS

Figure 3 shows the magnetic flux distribution in the starting and stead-state mode of induction motor operation for healthy and broken bars. The reasons for asymmetry of the flux lines are eddy current particularly in the slots of the rotor, sever changes of slip at the beginning of starting period and very high starting current (Fig. 3(a)). In addition injected harmonic currents and saturation due to the broken bars also cause asymmetry of the flux lines (Fig. 3(c)).When the healthy induction motor approaches the steady-state, the flux lines are more symmetrical distributed (Fig. 3(b)), while in broken bar motor the flux lines

distribution are still unsymmetrical in the steady-state mode (Fig. 3(d)).

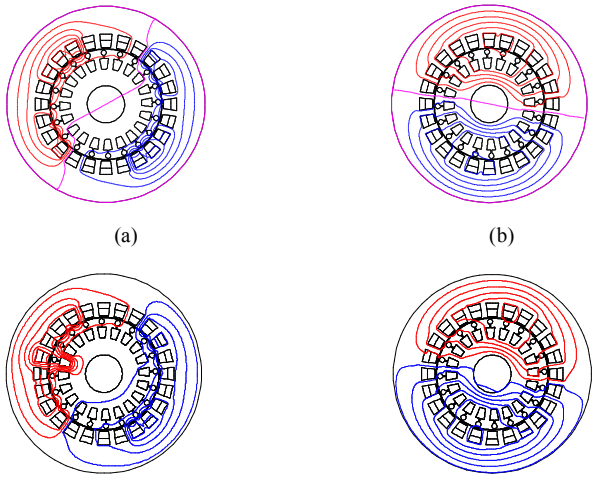

(a) (b)

(c) (d)

Fig.3. Flux distribution: (a) beginning of healthy motor starting, (b) steady-state operation of healthy motor, (c) beginning of faulty motor starting, (d) steady-state operation of faulty motor.

The current densities in the neighboured rotor bars to those broken are significantly increased (Fig.4.).

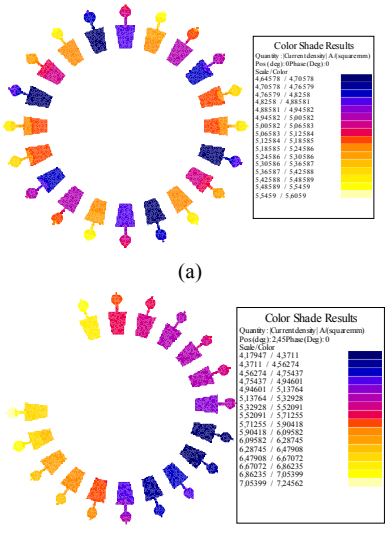

(a)

(b)

Fig.4. shaded plot of the component of the electric current density. (a) Healthy motor (b) motor with 3 Brocken bars.

IV. ANALYSIS OF FAULTY MOTOR PERFORMANCE

The table I represents the influence of the broken rotor bar on the motor efficiency.

TABLE I. *Influence of increasing number of broken rotor bars* on *motor efficiency*

N° of broken rotor bars	M_{en} N.m	P_{2n} kW	P_{j1n} Watt	P_{j2n} Watt	cosφ	η
0	25.86	7.5	365 .1	277 .2	0.84	0.87
1	25.76	7.37	361.03	272.64	0.8403	0.85
2	25.24	7.12	357.77	263 .91	0.8292	0.846
3	24.98	6.81	348 .08	253.02	0.8014	0.843
4	23.68	6.38	332	237 .92	0.776	0.839
5	21 .94	5.89	316.73	220 .77	0.737	0.833

One notices the reduction in the motor efficiency and the cosφ according to broken bars number.

This degrades the steady-state torque characteristic of the induction motor progressively (Fig. 5).We have also investigated the dynamic response of induction motor with healthy and faulty rotor cage, which is important in high dynamic servo drives.

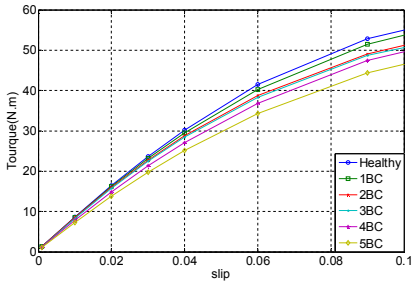

Fig.4. Influence of increasing number of broken rotor bars on induction motor performance— decreases of steady-state versus slip characteristic.

V. TRANSIENT ANALYSIS OF A FAULTY INDUCTION MOTOR

It is also possible to analyze the transient behavior of induction motor by the FEM. This is required in the control of induction motor in order to obtain the optimal time response. Meanwhile, the transient analysis of the motor is required for on-line fault diagnosis of the motor.

Fig. 6(a) shows time variations of phase a current for the three-phase healthy motor and no-load starting.
At the starting the current, flux and flux density are high and core saturates. If magnetization characteristic has not been included in the analysis of the starting of the motor, the teeth potential increases considerably. This leads to a large electromagnetic torques at the starting instant. However, analysis of the starting of the motor including the magnetization characteristic considerably reduces the developed torque compared with the constant permeability. In both cases the rate of

the torque variations is large due to the quick changes of the slip at the beginning of the starting.

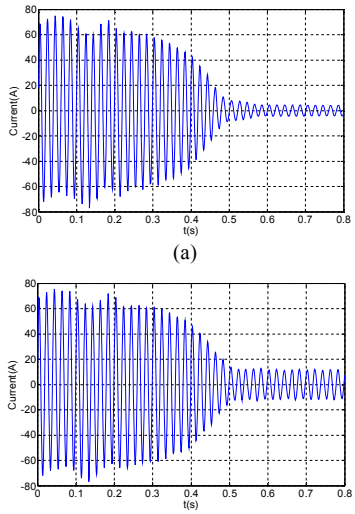

(a)

(b)

Fig.6. Time variations of current of a healthy induction motor: (a) Without load, (b) with full load.

Fig. 7 exhibits time variations of the torque, of a healthy no-load induction motor. The current of the bar just before the break passes the adjacent bars just after bar break.

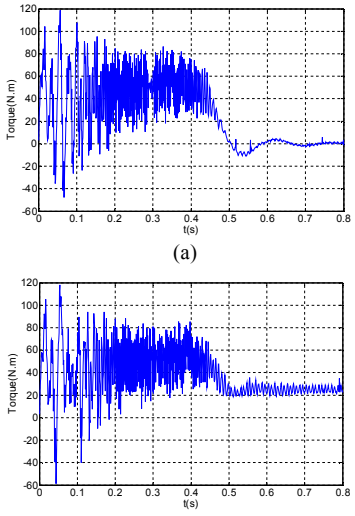

(a)

(b)

Fig.7. Time variations of torque of a healthy induction motor: (a) Without load,(b) with full load.

In addition to a deeper saturation of the core and the injected harmonics to the current, the RMS currents in the bars adjacent to the broken bar increase. However, raise of the broken bars leads to more serious problems in the motor.

Figs. 8(a) show the time variations of the current for 3 broken bars . More broken bars lead to more asymmetry of the magnetic flux density distribution which causes quick variations of the torque profiles (Fig. 9(a)). Starting of an on-load induction motor differs with that of the no-load motor. The starting period in this case is shorter that that of the no-load case. Meanwhile, instantaneous current, torque and speed at no-load are comparable with that of the full-load case. At the same time, difference between their steady-state cases is clearer.

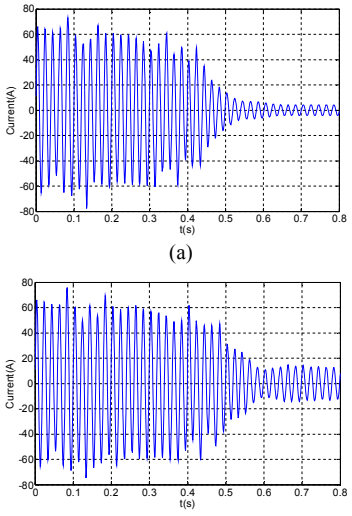

(a)

(b)

Fig.8. Time variations of current of a faulty induction motor, with 3 broken bars: (a) without load, (b) with full load.

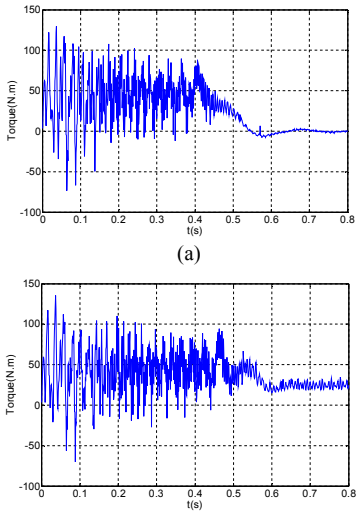

(a)

(b)

Fig.9.Time variations of torque of a faulty induction motor, with 3 broken bars: (a) without load, (b) with full load.

Fig. 6(b) show the time variations of a healthy on-load induction motor at starting. Figs. 8(b) exhibit the time variations of the on-load induction motor with 3 broken bars. Since the motor has been started on-load the steady-state torque must be equal to the rated speed (Fig. 9(b)).

The speed is less at the same load in the case of faulty rotor and it is visibly oscillating (Fig.10).

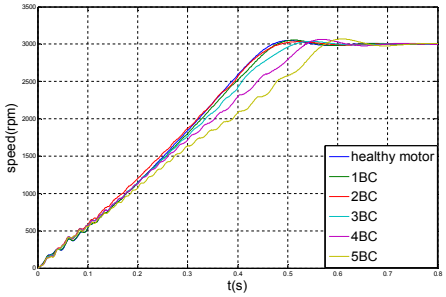

Fig. 10 Results of dynamic simulation for the healthy, respectively the faulty machine.

Fig. 11 shows the variations of the developed torque versus speed for healthy induction motor and motor with 3 broken bars.

A comparison of these results indicates that the rate of torque variations of the faulty motor is higher. The reason is the fault injects large harmonic components to the stator current which increase the amplitudes of the harmonic components. Therefore, the torque and speed of the faulty induction motor fluctuate and the rate of the faulty motor torque variations increases. So a higher noise and lower performance are expected from the faulty motor.

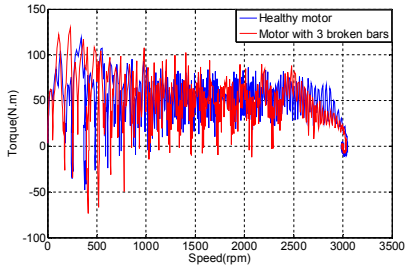

Fig. 11. Variations of torque versus speed for no-load.

It is of real interest to see what is happening in the rotor of the machine when broken bars appear. In Fig. 12 the currents through the rotor bar 4 (the next bar to those broken) are given.

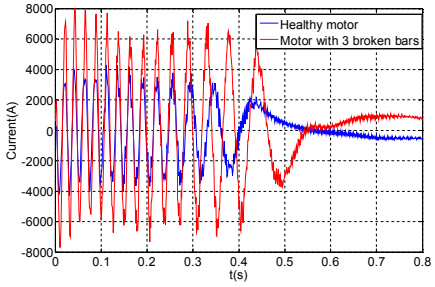

Fig.12. Current in rotor bar 4.

As it can be seen, the current in the neighbored bar of those broken is increased significantly.

VI. CONCLUSION

This paper analyzed a broken-bar voltage-fed three phase squirrel-cage induction motor in magneto harmonic and transient case.

FE computation was used for diagnosis and analysis of the broken rotor bars induction motor. The method has minimum simplifying assumptions and very high accuracy compared with other fault diagnosis methods. It has been shown that in broken bars motor the stator current characteristics and the torque are sensibility varied, the speed profiles oscillate.

The presented FEM analysis is one effective and inexpensive method for studying the influence of rotor faults on behavior of three phase squirrel-cage induction machines. The method has proved a significant applicability in the process of fault diagnosis of induction motors.

VIII. REFERENCES

[1] J. Faiz, B.M. Ebrahimi, Bilal Akin, H.A. Toliyat Finite-element transient analysis of induction motors under mixed eccentricity fault. *IEEE Trans Magn 2008;44(1):*66–74.

[2] J. Faiz, B.M. Ebrahimi, H.A. Toliyat ,W.S. Abu-Elhaija. Mixed-fault diagnosis in induction motors considering varying load and broken bars location. *J.Energy Conversion and Management.2010.*

[3] J. Faiz, B.M. Ebrahimi, Bilal Akin, H.A.Toliyat. Comprehensive eccentricity fault diagnosis in induction motors using finite element. Trans Magn 2009;45(3).

[4] JF. Bangura,RJ. Povinelli, NAO. Demerdash, RH.Brown: Diagnostics of eccentricities and bar/end-ring connector breakages in poly phase induction motors through a combination of time series data mining and time-stepping coupled FE-state-space techniques industry applications. *IEEE Trans Ind Appl 2003;39(4):*1005–13.

[5] L. SZABÓ, J.B. DOBAI, and K.A. BIRÓ: FEM based transient motion analysis of induction machines having broken rotor bars, Proceedings of 2007 IEEE-TTTC International Conference on Automation, Quality and Testing, Robotics, Cluj (Romania), 2007, pp 353-358.

[7] T. Tudorache, L. Melcescu and V. Petre: High Efficiency Squirrel Cage Induction Machines. International Conference on Renewable Energies and Power Quality (ICREPQ'09) ,Valencia (Spain), 15th to 17th April, 2009.